

High- and low-energy constraints on top-Higgs couplings

W. Dekens*

Los Alamos National Laboratory, New Mexico Consortium

E-mail: wdekens@newmexicoconsortium.org

We study the five chirality-flipping interactions that appear in the top-Higgs sector at leading order in the standard model effective field theory. We consider constraints from collider observables, flavor physics, and electric-dipole-moment experiments. This analysis results in very competitive constraints from indirect observables when one considers a single coupling at a time. In addition, we discuss how these limits are affected in scenarios in which multiple top-Higgs interactions are generated at the scale of new physics.

*9th International Workshop on the CKM Unitarity Triangle
28 November - 3 December 2016
Tata Institute for Fundamental Research (TIFR), Mumbai, India*

*Speaker.

1. Introduction

As the top quark has the largest coupling to the Higgs boson, and thereby the electroweak symmetry breaking sector, it might be the most sensitive to influences of new physics. This is exemplified in several beyond-the-standard-model (BSM) scenarios relevant for baryogenesis [1–4]. In these cases one expects enhanced deviations from the SM to occur in the interactions of the top quark and the Higgs boson. These top-Higgs couplings can be probed directly by measurements of processes involving top quarks at the LHC. Other, ‘indirect’, constraints come from processes which do not involve the top quark, but to which the top-Higgs couplings can contribute through loop corrections. As we will discuss, such indirect observables can give rise to complementary constraints, and, in some cases, are more stringent than the direct limits.

In the following we discuss direct and indirect limits on dimension-six chirality-flipping top-Higgs interactions within the framework of the standard model effective field theory (SM-EFT). We do not consider chirality conserving top-Higgs operators, for recent analyses see e.g. [5–7], which only mix with the top-Higgs couplings at three loops [8–10]. We introduce the chirality-flipping operators in section 2. An overview of their contributions to direct observables (such as single-top, $t\bar{t}$, and $t\bar{t}h$ production) and indirect collider observables ($gg \leftrightarrow h$, $h \rightarrow \gamma\gamma$) is given in section 3. Observables in flavor physics (such as $B \rightarrow X_s \gamma$) and electric dipole moment (EDM) searches are discussed in sections 4 and 5. We consider the resulting limits, and discuss how these constraints are affected when all couplings are turned on at the same time, in section 6.

2. Operator structure

Assuming that new physics arises at a scale Λ well above the electroweak scale, $\Lambda \gg v$ where $v \simeq 246$ GeV, BSM effects can be described by higher-dimensional operators in the SM-EFT. Here we keep only effects linear in v^2/Λ^2 which can be described by the minimal set of dimension-six operators that has been derived in [11, 12]. If we further assume that the dominant BSM effects appear in the chirality-flipping top-Higgs sector, the dimension-six Lagrangian involves five operators,

$$\mathcal{L}_{\text{top}} = \sum_{\alpha \in \{Y, g, \gamma, Wt, Wb\}} C_\alpha O_\alpha + \text{h.c.} \quad (2.1)$$

where $C_\alpha = c_\alpha + i\tilde{c}_\alpha$ are complex couplings. In the unitary gauge and in the quark mass basis the operators are given by,

$$O_\gamma = -\frac{eQ_t}{2} m_t \bar{t}_L \sigma_{\mu\nu} (F^{\mu\nu} - t_W Z^{\mu\nu}) t_R \left(1 + \frac{h}{v}\right), \quad (2.2)$$

$$O_g = -\frac{g_s}{2} m_t \bar{t}_L \sigma_{\mu\nu} G^{\mu\nu} t_R \left(1 + \frac{h}{v}\right), \quad (2.3)$$

$$O_{Wt} = -gm_t \left[\frac{1}{\sqrt{2}} \bar{b}'_L \sigma^{\mu\nu} t_R W_{\mu\nu}^- + \bar{t}_L \sigma^{\mu\nu} t_R \left(\frac{1}{2c_W} Z_{\mu\nu} + igW_\mu^- W_\nu^+ \right) \right] \left(1 + \frac{h}{v}\right), \quad (2.4)$$

$$O_{Wb} = -gm_b \left[\frac{1}{\sqrt{2}} \bar{t}'_L \sigma^{\mu\nu} b_R W_{\mu\nu}^+ - \bar{b}_L \sigma^{\mu\nu} b_R \left(\frac{1}{2c_W} Z_{\mu\nu} + igW_\mu^- W_\nu^+ \right) \right] \left(1 + \frac{h}{v}\right), \quad (2.5)$$

$$O_Y = -m_t \bar{t}_L t_R \left(vh + \frac{3}{2} h^2 + \frac{1}{2} \frac{h^3}{v} \right), \quad (2.6)$$

where $F_{\mu\nu}$, $Z_{\mu\nu}$, $W_{\mu\nu}^\pm$, and $G_{\mu\nu}^a$ are the field strengths of the photon, Z boson, W^\pm boson, and gluon, while e , g , and g_s denote the $U(1)_{\text{EM}}$, $SU(2)$ and $SU(3)_c$ gauge couplings, respectively. Furthermore, h represents the Higgs field, $Q_t = 2/3$, $t_W = \tan \theta_W$, $c_W = \cos \theta_W$, with θ_W the Weinberg angle. Finally, the operators O_{W_t, W_b} contain the combinations $b' = V_{tb}b + V_{ts}s + V_{td}d$, and $t' = V_{tb}^*t + V_{cb}^*c + V_{ub}^*u$, where V_{ij} represent the SM CKM elements. These operators, in the mass basis, can be related to the $SU(2) \times U(1)_Y$ invariant operators of [11, 12] as discussed in Refs. [13, 14]. Furthermore, at low energies the first of the above operators can be interpreted as the electric and magnetic dipole moments of the top quark, ($d_t = (em_t Q_t)\tilde{c}_\gamma$ and $\mu_t = (em_t Q_t)c_\gamma$). The second is related to the non-abelian gluonic electric and magnetic dipole moments, ($\tilde{d}_t = m_t \tilde{c}_g$ and $\tilde{\mu}_t = m_t c_g$).

In what follows we will assume that the operators in Eqs. (2.2) - (2.6) capture the dominant BSM effects, and therefore set all other dimension-six operators to zero at the scale Λ . However, the renormalization group evolution (RGE), as well as threshold effects, will induce additional dimension-six operators. As we will see below, these additional operators will lead to stringent constraints from indirect observables.

3. Collider observables and electroweak precision tests

The operators in Eqs. (2.2) - (2.6) can be probed directly in the production and decay of top quarks. Of the observables in the former category we consider single top [14], $t\bar{t}$ [15, 16], and $t\bar{t}h$ [17, 18] production, while we study the W helicity fractions in $t \rightarrow Wb$ decays [19]. These processes receive corrections from the top-Higgs couplings at tree level. In particular, single top production and the helicity fractions are sensitive to corrections to the Wtb vertex generated by C_{W_t} . Both $t\bar{t}$ and $t\bar{t}h$ production receive corrections from the gluonic dipole moment, C_g , while the top Yukawa, C_Y only affects $t\bar{t}h$. We summarize which of the observables receive contributions from the top-Higgs couplings in the left panel of Table 1.

At the one-loop level, the C_α couplings can also contribute to processes without a top quark in the final state. Examples of such indirect observables are electroweak precision tests, namely the S parameter, and Higgs production and decay signal strengths, in particular, $h \leftrightarrow gg$, and $h \rightarrow \gamma\gamma$. Both Higgs production and decay channels are induced at loop-level in the SM, such that the loop generated BSM contributions can be sizable in comparison. These contributions are induced by the following additional Higgs-gauge operators

$$O_{\phi\gamma} = e^2 F_{\mu\nu} F^{\mu\nu} \phi^\dagger \phi, \quad O_{\phi G} = g_s^2 G_{\mu\nu}^a G^{a,\mu\nu} \phi^\dagger \phi, \quad O_{\phi WB} = gg' W_{\mu\nu}^I B^{\mu\nu} \phi^\dagger \tau^I \phi \quad (3.1)$$

where ϕ is the Higgs doublet and $B_{\mu\nu}$ (g') is the $U(1)_Y$ field strength (coupling constant), and $B_\mu = c_W A_\mu - s_W Z_\mu$. The C_γ and C_g couplings induce the $O_{\phi\gamma}$ and $O_{\phi G}$ operators through RG evolution between $\mu = \Lambda$ and $\mu = m_H$ [8–10], while C_Y induces both operators through threshold effects. The additional operator $O_{\phi WB}$ is generated by C_γ and C_{W_t} . In turn, $O_{\phi\gamma}$ and $O_{\phi G}$ contribute to $h \rightarrow \gamma\gamma$ and $h \leftrightarrow gg$, while $O_{\phi WB}$ induces the S parameter. These contributions are summarized in the right panel of Table 1.

As we only consider effects linear in v^2/Λ^2 , we do not take into account contributions that are quadratic in the top-Higgs couplings. This implies that measurements of cross sections are only

		Obs.	C_γ	C_g	C_{Wt}	C_{Wb}	C_Y
Direct	t	\times	\times	\checkmark	\times	\times	
	$t\bar{t}$	\times	\checkmark	\times	\times	\times	
	$t\bar{t}h$	\times	\checkmark	\times	\times	\checkmark	
	$t \rightarrow Wb$	\times	\times	\checkmark	\times	\times	

		Obs.	C_γ	C_g	C_{Wt}	C_{Wb}	C_Y
Indirect	$gg \leftrightarrow h$	\times	$O_{\phi G}$	\times	\times	\times	$O_{\phi G}$
	$h \rightarrow \gamma\gamma$	$O_{\phi\gamma}$	\times	\times	\times	\times	$O_{\phi\gamma}$
	S	$O_{\phi WB}$	\times	$O_{\phi WB}$	\times	\times	\times

Table 1: The left and right panels give an overview of the contributions of the top-Higgs couplings to direct and indirect observables, respectively. A \checkmark indicates a direct (tree-level) contribution and \times a negligible contribution. The O_i indicate indirect contributions induced through the additional operator O_i defined in Eq. (3.1).

sensitive to the real parts of C_α . Of the above mentioned observables only the phase δ^- , which is measured in $t \rightarrow Wb$ decays [20, 21], is sensitive to the imaginary part of C_{Wt} .

4. Flavor physics

At scales $\mu \simeq m_b$ the top-Higgs couplings give rise to (flavor-changing) interactions that can, in principle, be probed in multiple flavor observables. Here we focus on the flavor-changing $B \rightarrow X_s \gamma$ transitions which give rise to the most stringent constraints. We consider the branching ratio and the CP-asymmetry, both of which are induced by the dipole operators O_7 and O_8 [22–24],

$$O_7 = \frac{e}{16\pi^2} m_b \bar{s}_L \sigma^{\mu\nu} F_{\mu\nu} b_R, \quad O_8 = -\frac{g_s}{16\pi^2} m_b \bar{s}_L \sigma^{\mu\nu} G_{\mu\nu}^a t^a b_R, \quad (4.1)$$

which appear in the Lagrangian, $\mathcal{L}_{b \rightarrow s} = -4V_{tb}V_{ts}^* G_F / \sqrt{2} \sum_{i=7,8} C_i O_i$. These two operators are induced through the RG evolution from the scale Λ to the b quark mass scale. All top-Higgs operators, apart from the top Yukawa C_Y , contribute to these operators through one-loop diagrams, although the resulting constraints are most relevant for C_{Wt} and C_{Wb} . The combination of the branching ratio and the CP asymmetry then leads to constraints on the real and imaginary parts of these top-Higgs couplings.

5. Electric dipole moments

EDMs are generated by additional operators that the top-Higgs couplings induce through loop effects. The set of additional operators that give rise to EDMs at low energies, $\mu \sim 2$ GeV, is given by

$$\begin{aligned} \mathcal{L}_{\text{EDM}} = & -\frac{i}{2} \sum_{q=u,d,s,c,b} \left[e Q_q m_q C_\gamma^{(q)} \bar{q} \sigma^{\mu\nu} \gamma_5 q F_{\mu\nu} + g_s m_q C_g^{(q)} \bar{q} \sigma^{\mu\nu} \gamma_5 t^a q G_{\mu\nu}^a \right] \\ & + C_{\tilde{G}} \frac{g_s}{3} f_{abc} \tilde{G}^{a\mu\nu} G_{\mu\rho}^b G_{\nu\rho}^c - \frac{i}{2} e Q_e m_e C_\gamma^{(e)} \bar{e} \sigma^{\mu\nu} \gamma_5 e F_{\mu\nu}, \end{aligned} \quad (5.1)$$

where $\tilde{G}_{\mu\nu}^a = \frac{1}{2} \epsilon_{\mu\nu\alpha\beta} G^{a\alpha\beta}$. The operators in the first line are the quark EDMs and quark color-EDMs and the first term in the second line represents the CP-odd three-gluon operator, all of which

Obs.	\tilde{c}_γ	\tilde{c}_g	\tilde{c}_{Wt}	\tilde{c}_{Wb}	\tilde{c}_Y
d_{ThO}	$O_{\phi\tilde{X},lequ} \rightarrow O_\gamma^{(e)}$	$O_\gamma \rightarrow O_{\phi\tilde{X},lequ} \rightarrow O_\gamma^{(e)}$	$O_{\phi\tilde{X},lequ} \rightarrow O_\gamma^{(e)}$	\mathbf{X}	$O_\gamma^{(e)}$
d_n, d_{Hg}	$O_{\phi\tilde{X},quqd} \rightarrow O_{\gamma,g}^{(q)}$	$O_{\tilde{G}}$	$O_{\phi\tilde{X},quqd} \rightarrow O_{\gamma,g}^{(q)}$	$O_g^{(b)} \rightarrow O_{\tilde{G}}$	$O_{\gamma,g}^{(q)}, O_{\tilde{G}}$

Table 2: The Table gives an overview of the contributions of the top-Higgs couplings to EDMs. \mathbf{X} indicates a negligible contribution. The other entries illustrate the mechanism through which the dominant contributions arise and the additional operators (defined in Eqs. (5.1) and (5.2)) that are induced in the process.

induce the EDMs of nucleons and nuclei. These EDMs can be calculated by first performing the nonperturbative matching to an extension of chiral perturbation theory that incorporates CPV hadronic interactions [25,26]. The EDMs of the nucleons, d_n and d_p , can then be expressed in terms of these CPV hadronic interactions, while for nuclear systems, such as ^{199}Hg , nuclear-structure calculations are required to do so. Both the matching to chiral effective theory and the nuclear calculations involve significant uncertainties. The theoretical errors are under control in the case of the contributions of the quark EDMs to $d_{n,p}$, due to lattice calculations with $\mathcal{O}(15\%)$ uncertainties [27–29], while calculations for the color-EDMs are underway [30,31]. Moving on from the quark EDMs, other uncertainties range from $\mathcal{O}(50\%)$, for the contributions of the color-EDMs to $d_{n,p}$, to over 100% with an unknown sign, in case of the dependence of d_{Hg} on the CPV pion-nucleon couplings. In contrast, the measurement of the ThO molecule, d_{ThO} , has a rather clean theoretical interpretation in terms of the electron EDM (last operator in Eq. (5.1)). For reviews of these issues see e.g. [32,33]. Here we will employ the EDM measurements of the neutron, ThO, and mercury [34–36]. We briefly comment on the impact of theory errors in section 6, see [14,37] for details.

To generate d_n , d_{ThO} and d_{Hg} one first has to induce the operators in Eq. (5.1). C_Y generates all operators through two-loop Barr-Zee diagrams [38,39], while C_g (C_{Wb}) does so at the one (two) loop level by inducing the $O_{\tilde{G}}$ operator. The operators $O_{\gamma,Wt}$ can also induce EDMs at one loop, however, such contributions are generated through a W loop which involves a small factor of $|V_{ub}|^2$. In addition, these diagrams only generate the quark (color-)EDMs and do not induce the, experimentally more stringently constrained, electron EDM. As a result, a two-loop mechanism gives rise to limits on $O_{\gamma,Wt}$ which are stronger by roughly three orders of magnitude [13,14]. In this mechanism, one-loop RG evolution first induces additional operators, which are not present in Eq. (5.1), namely,

$$\begin{aligned}
 \mathcal{L}'_{\text{EDM}} = \phi^\dagger & \left[C_{\phi\tilde{B}} g'^2 B^{\mu\nu} \tilde{B}_{\mu\nu} + C_{\phi\tilde{W}} g^2 W^{I\mu\nu} \tilde{W}_{\mu\nu}^I + C_{\phi\tilde{W}B} g g' B^{\mu\nu} \tau \cdot \tilde{W}_{\mu\nu} + C_{\phi\tilde{G}} g_s^2 G^{a\mu\nu} \tilde{G}_{\mu\nu}^a \right] \phi \\
 & + C_{lequ} (\tilde{l}_L^I \sigma^{\mu\nu} e_R) \varepsilon_{IJ} (\tilde{q}_L^J \sigma_{\mu\nu} u_R) \\
 & + C_{quqd}^{(1)} (\tilde{q}_L^I \sigma^{\mu\nu} u_R) \varepsilon_{IJ} (\tilde{q}_L^J \sigma_{\mu\nu} d_R) + C_{quqd}^{(8)} (\tilde{q}_L^I \sigma^{\mu\nu} t^a u_R) \varepsilon_{IJ} (\tilde{q}_L^J \sigma_{\mu\nu} t^a d_R). \quad (5.2)
 \end{aligned}$$

In the second step a subset of the above operators, $C_{\phi\tilde{W}B, \phi\tilde{W}, \phi\tilde{B}, lequ}$, generates the electron EDM through an additional loop. In similar fashion, $C_{\phi\tilde{G}}$ and $C_{quqd}^{(1,8)}$ generate the quark (color-)EDMs and thereby hadronic EDMs. Since all of the operators in Eq. (5.2) are induced by $O_{\gamma,Wt}$, the stronger experimental limit on the electron EDM gives the most stringent bounds on these top-Higgs couplings. The contributions of all top-Higgs couplings, and the mechanisms by which they do so, are summarized in Table 2.

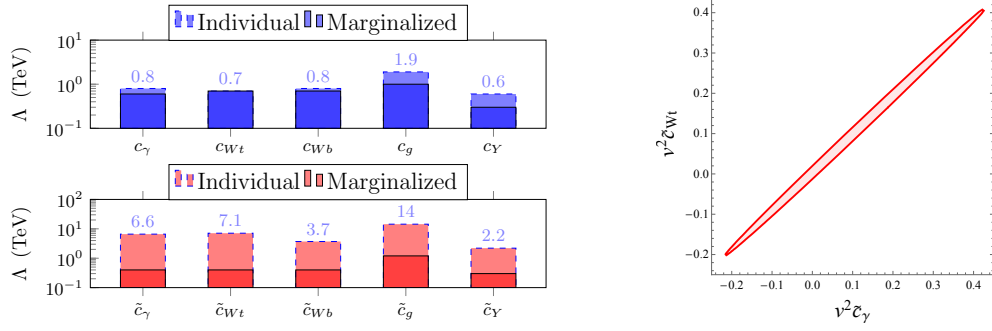


Figure 1: The solid bars in the left panel show the constraints on each operator, C_α , after marginalizing over the other operators. The dashed bars give the limits assuming only one operator is present. The limits are naively translated to a scale of new physics by using $C_\alpha = v^2/\Lambda^2$. The right panel shows the limits in the $v^2 \tilde{c}_\gamma - v^2 \tilde{c}_{Wt}$ plane after marginalizing over the other couplings.

6. Discussion

We summarize the constraints that result from the above outlined analysis in Fig. 1. Here the top and bottom panels on the left show the limits on the real and imaginary parts, respectively. The dashed bars indicate the bounds in the scenario that a single top-Higgs coupling is turned on at the high scale. One can see that the limits on the imaginary parts are generally stronger than those on the real parts (note the different scales in Fig. 1). In this scenario the limits on the real part of C_{Wb} comes from $B \rightarrow X_s \gamma$, while the limits on C_γ , C_g , and C_Y arise mainly from the indirect collider observables $h \rightarrow \gamma\gamma$ and $gg \leftrightarrow h$. The bound on the real part of C_{Wt} is dominated by the direct observables in $t \rightarrow Wb$. The limits on all imaginary parts are dominated by EDMs, $C_{\gamma, Wt, Y}$ are stringently constrained by d_{ThO} while the stronger constraints on $C_{g, Wb}$ come from d_n and d_{Hg} . The constraints resulting from d_{ThO} are hardly affected by the theory uncertainties mentioned in section 5, while those from d_n and d_{Hg} weaken significantly. The limit on C_g (C_{Wb}) is weakened by two (one) order of magnitude if one uses the ‘Rfit’ approach [40] for these uncertainties.

The solid bars in Fig. 1 give the limits in the scenario when all five operators are present at the scale Λ . As can be seen from the left panel, the real parts are mildly affected, while the limits on the imaginary parts are drastically weakened. This is due to significant cancellations between different contributions to the EDMs. As an example of this we show the $\tilde{c}_\gamma - \tilde{c}_{Wt}$ plane in the right panel of Fig. 1. Here the ThO measurement limits the couplings to the diagonal band. However, this indirect observable alone allows for a free direction, which is only ruled out by direct probes (the helicity fractions). This further motivates collider observables which are directly sensitive to CP violation such as the ones proposed in [41–43].

Acknowledgments

I would like to thank the organizers of the CKM2016 workshop, in particular the conveners of Working Group 6, for an interesting and enjoyable meeting. I am grateful to Vincenzo Cirigliano, Emmanuele Mereghetti, and Jordy de Vries for the collaboration on this work. This work was supported by the Dutch Organization for Scientific Research (NWO) through a RUBICON grant.

References

- [1] D. B. Kaplan, Nucl. Phys. **B365**, 259 (1991).
- [2] K. Agashe, G. Perez, and A. Soni, Phys. Rev. **D75**, 015002 (2007), hep-ph/0606293.
- [3] M. Carena, G. Nardini, M. Quiros, and C. E. M. Wagner, Nucl. Phys. **B812**, 243 (2009), 0809.3760.
- [4] A. Kobakhidze, L. Wu, and J. Yue, JHEP **10**, 100 (2014), 1406.1961.
- [5] C. Hartmann, W. Shepherd, and M. Trott, (2016), 1611.09879.
- [6] A. Buckley *et al.*, JHEP **04**, 015 (2016), 1512.03360.
- [7] S. Alioli, V. Cirigliano, W. Dekens, J. de Vries, and E. Mereghetti, (2017), 1703.04751.
- [8] E. E. Jenkins, A. V. Manohar, and M. Trott, JHEP **10**, 087 (2013), 1308.2627.
- [9] E. E. Jenkins, A. V. Manohar, and M. Trott, JHEP **01**, 035 (2014), 1310.4838.
- [10] R. Alonso, E. E. Jenkins, A. V. Manohar, and M. Trott, JHEP **04**, 159 (2014), 1312.2014.
- [11] W. Buchmüller and D. Wyler, Nucl. Phys. B **268**, 621 (1986).
- [12] B. Grzadkowski and M. Misiak, Phys. Rev. D **78**, 077501 (2008), 0802.1413.
- [13] V. Cirigliano, W. Dekens, J. de Vries, and E. Mereghetti, Phys. Rev. **D94**, 016002 (2016), 1603.03049.
- [14] V. Cirigliano, W. Dekens, J. de Vries, and E. Mereghetti, Phys. Rev. **D94**, 034031 (2016), 1605.04311.
- [15] D. Atwood, A. Kagan, and T. G. Rizzo, Phys. Rev. **D52**, 6264 (1995), hep-ph/9407408.
- [16] P. Haberl, O. Nachtmann, and A. Wilch, Phys. Rev. **D53**, 4875 (1996), hep-ph/9505409.
- [17] C. Degrande, J. M. Gerard, C. Grojean, F. Maltoni, and G. Servant, JHEP **07**, 036 (2012), 1205.1065, [Erratum: JHEP03,032(2013)].
- [18] A. Hayreter and G. Valencia, Phys. Rev. **D88**, 034033 (2013), 1304.6976.
- [19] J. Drobnak, S. Fajfer, and J. F. Kamenik, Phys. Rev. **D82**, 114008 (2010), 1010.2402.
- [20] J. Boudreau, C. Escobar, J. Mueller, K. Sapp, and J. Su, (2013), 1304.5639.
- [21] ATLAS, G. Aad *et al.*, JHEP **04**, 023 (2016), 1510.03764.
- [22] E. Lunghi and J. Matias, JHEP **04**, 058 (2007), hep-ph/0612166.
- [23] A. L. Kagan and M. Neubert, Eur. Phys. J. **C7**, 5 (1999), hep-ph/9805303.
- [24] M. Benzke, S. J. Lee, M. Neubert, and G. Paz, Phys. Rev. Lett. **106**, 141801 (2011), 1012.3167.
- [25] J. de Vries, E. Mereghetti, R. G. E. Timmermans, and U. van Kolck, Annals Phys. **338**, 50 (2013), 1212.0990.
- [26] J. Bsaisou, U.-G. Meißner, A. Nogga, and A. Wirzba, Annals Phys. **359**, 317 (2015), 1412.5471.
- [27] T. Bhattacharya, V. Cirigliano, R. Gupta, H.-W. Lin, and B. Yoon, Phys. Rev. Lett. **115**, 212002 (2015), 1506.04196.
- [28] PNDME, T. Bhattacharya *et al.*, Phys. Rev. **D92**, 094511 (2015), 1506.06411.
- [29] T. Bhattacharya *et al.*, Phys. Rev. **D94**, 054508 (2016), 1606.07049.

- [30] T. Bhattacharya, V. Cirigliano, R. Gupta, and B. Yoon, Quark Chromoelectric Dipole Moment Contribution to the Neutron Electric Dipole Moment, in *Proceedings, 34th International Symposium on Lattice Field Theory (Lattice 2016): Southampton, UK, July 24-30, 2016*, 2016, 1612.08438.
- [31] M. Abramczyk *et al.*, (2017), 1701.07792.
- [32] J. Engel, M. J. Ramsey-Musolf, and U. van Kolck, *Prog. Part. Nucl. Phys.* **71**, 21 (2013), 1303.2371.
- [33] N. Yamanaka *et al.*, (2017), 1703.01570.
- [34] C. A. Baker *et al.*, *Phys. Rev. Lett.* **97**, 131801 (2006), hep-ex/0602020.
- [35] ACME Collaboration, J. Baron *et al.*, *Science* **343**, 269 (2014), 1310.7534.
- [36] B. Graner, Y. Chen, E. G. Lindahl, and B. R. Heckel, (2016), 1601.04339.
- [37] Y. T. Chien, V. Cirigliano, W. Dekens, J. de Vries, and E. Mereghetti, *JHEP* **02**, 011 (2016), 1510.00725, [JHEP02,011(2016)].
- [38] S. M. Barr and A. Zee, *Phys. Rev. Lett.* **65**, 21 (1990).
- [39] J. Gunion and D. Wyler, *Phys.Lett.* **B248**, 170 (1990).
- [40] CKMfitter Group, J. Charles *et al.*, *Eur. Phys. J.* **C41**, 1 (2005), hep-ph/0406184.
- [41] A. Prasath V, R. M. Godbole, and S. D. Rindani, *Eur. Phys. J.* **C75**, 402 (2015), 1405.1264.
- [42] F. Boudjema, R. M. Godbole, D. Guadagnoli, and K. A. Mohan, *Phys. Rev.* **D92**, 015019 (2015), 1501.03157.
- [43] N. Mileo, K. Kiers, A. Szynekman, D. Crane, and E. Gegner, (2016), 1603.03632.